Noncollinear magnetic ordering in small chromium clusters

C. Kohl and G. F. Bertsch
Institute for Nuclear Theory–Department of Physics, University of Washington, Seattle, Washington 98195
(Received 16 February 1999)

We investigate noncollinear effects in antiferromagnetically coupled clusters using the general, rotationally invariant form of local spin-density theory. The coupling to the electronic degrees of freedom is treated with relativistic nonlocal pseudopotentials and the ionic structure is optimized by Monte Carlo techniques. We find that small chromium clusters ($N \leqslant 13$) strongly favor noncollinear configurations of their local magnetic moments due to frustration. This effect is associated with a significantly lower total magnetization of the noncollinear ground states, ameliorating the disagreement between Stern-Gerlach measurements and previous collinear calculations for Cr_{12} and Cr_{13}. Our results further suggest that the trend to noncollinear configurations might be a feature common to most antiferromagnetic clusters. [S0163-1829(99)10929-9]

I. INTRODUCTION

Magnetic properties of transition-metal clusters have become the subject of intensive research, both from the experimental[1–4] and theoretical point of view.[5–8] One of the most interesting and challenging aspects of that field is the subtle interplay between geometric structure and magnetic ordering that has mostly been investigated for ferromagnetic $3d$ clusters and $4d$ clusters. Finite-size effects and a reduced dimensionality often lead to a significantly different magnetic behavior from the bulk with clusters having enhanced atomic moments,[9,10] larger anisotropy energies,[11] or an altered temperature dependence of the magnetization.[12]

Almost all theory to date employed the local spin-density approximation (LSDA) with the assumption that the spin-density matrix is diagonal in some particular frame. In that special case, the spins are automatically collinear along a fixed quantization axis. The only generalized spin-density calculation for clusters that treats the electron spin as a vector observable and a function of position has recently been performed by Car and co-workers.[13] They have shown that noncollinear configurations exist in Fe_3 and Fe_5, although the effect on structure and energetics of these ferromagnetic (FE) clusters is not very pronounced. On the other hand, an unconstrained orientation of the quantization axis is known to play a key role in describing various nonferromagnetic systems like the γ phase of bulk iron,[14] disordered systems,[15] or ultrathin Fe films with a partial antiferromagnetic (AF) coupling.[16] Furthermore, the work on Fe/Cr (Ref. 17) and Ag/Cr multilayers[18] demonstrated how the competition between AF ordering and frustration of the Cr moments leads to noncollinear arrangements in the form of a spin-density wave. Although the importance of frustration in AF systems seems to be evident and was discussed in detail for embedded Cr clusters by Pastor and co-workers,[19] and more generally by Manninen and co-workers,[20] the possibility of noncollinear effects has not yet been considered for AF clusters.

In this paper, we present a general local spin-density calculation for clusters of AF materials. Besides the motivation given above, we have decided to explore noncollinear effects in chromium clusters for two reasons: First, chromium is particularly challenging amongst the $3d$ elements due to its maximal spin alignment in the atom ($3d^5 4s^1$): all valence electrons have parallel spins, i.e., the total magnetization is $S=3$. This leads to a variety of unique effects including an unusually short dimer bonding length or a repulsion for FE coupling at small distances.[21] The other reason why we chose chromium is the possibility to compare with the thorough *ab initio* study of Cr clusters by Cheng and Wang.[22] These authors recently employed the conventional LSDA for $N_{at} \leqslant 15$, finding all clusters to be antiferromagnetically coupled. Their structures can serve as a benchmark to check our computations concerning the restriction to collinear configurations—an aspect that is crucial to extract the importance of noncollinear effects.

In Sec. II we outline the fundamentals of our theoretical approach and briefly motivate the structure optimization. This involves the rotationally invariant LSDA to find the electronic ground state and a relativistic, nonlocal pseudopotential for their interaction with the ions. In Sec. III we discuss some numerical tests and present our results. We find noncollinear spin configurations for all investigated clusters. We demonstrate the influence of noncollinearity on the geometry and on the total magnetic moment and discuss how this reduces the discrepancy concerning the magnetization of some chromium clusters between the experiment by Bloomfield and co-workers[23] and some previous theoretical results.[22,24]

II. THEORETICAL AND NUMERICAL BACKGROUND

The density-functional theory in its most general form, as developed by Barth and Hedin,[25] allows the orientation of each spin to vary with position. The wave functions are described by complex two-component spinors $\Psi=(\Psi_\sigma,\Psi_{\sigma'})$, where σ and σ' denote the spin indices, and the degrees of freedom are the elements of the single-particle spin-density matrix

$$\rho_{\sigma\sigma'}(\vec{r})=\sum_i \Psi_{i,\sigma}(\vec{r})\Psi^*_{i,\sigma'}(\vec{r}). \tag{1}$$

Assuming this matrix to be diagonal, the usual local spin-density functionals are parameterized in terms of $\rho_{\uparrow\uparrow}(\vec{r})$

$=:\rho_{\uparrow}(\vec{r})$ and $\rho_{\downarrow\downarrow}(\vec{r})=:\rho_{\downarrow}(\vec{r})$ only. In that special case, the spins are necessarily collinear along the chosen quantization axis and the exchange-correlation potential is obtained via $V_{\sigma}^{\mathrm{xc}}=\partial E^{\mathrm{xc}}[\rho_{\uparrow},\rho_{\downarrow}]/\partial\rho_{\sigma}$. However, rotational invariance requires that the true variables are the eigenvalues $n_{\uparrow}(\vec{r})$ and $n_{\downarrow}(\vec{r})$ of the spin-density matrix $\rho_{\sigma\sigma'}(\vec{r})$. We can thus apply standard local spin-density functionals (we chose the formula of Perdew and Wang[26]) by evaluating the potential in a locally diagonal frame. The transformation is carried out following the work of Kübler *et al.*[27] who used the spin-1/2 rotation matrix

$$\hat{U}(\vec{r})=\begin{pmatrix} \cos\frac{\theta(\vec{r})}{2}e^{(i/2)\phi(\vec{r})} & \sin\frac{\theta(\vec{r})}{2}e^{(-i/2)\phi(\vec{r})} \\ -\sin\frac{\theta(\vec{r})}{2}e^{(i/2)\phi(\vec{r})} & \cos\frac{\theta(\vec{r})}{2}e^{(-i/2)\phi(\vec{r})} \end{pmatrix} \tag{2}$$

to locally diagonalize the spin-density matrix:

$$\sum_{\sigma\sigma'} U_{\alpha\sigma}(\vec{r})\rho_{\sigma\sigma'}(\vec{r})U^{*}_{\sigma'\beta}(\vec{r})=\delta_{\alpha\beta}n_{\alpha}(\vec{r}). \tag{3}$$

By working in this representation we express $\partial E^{\mathrm{xc}}/\partial\rho_{\sigma\sigma'}$ by $E^{\mathrm{xc}}/\partial n_{\sigma}$ plus the introduction of local spin rotation angles $\phi(\vec{r})$ and $\theta(\vec{r})$ that are the local azimuthal and polar angles of the magnetization density vector. They are computed from Eq. (3) through the requirement of vanishing off-diagonal elements as

$$\phi(\vec{r})=-\tan^{-1}\frac{\mathrm{Im}\,\rho_{\uparrow\downarrow}(\vec{r})}{\mathrm{Re}\,\rho_{\uparrow\downarrow}(\vec{r})},$$

$$\theta(\vec{r})=\tan^{-1}\frac{2\{[\mathrm{Re}\,\rho_{\uparrow\downarrow}(\vec{r})]^2+[\mathrm{Im}\,\rho_{\uparrow\downarrow}(\vec{r})]^2\}^{1/2}}{\rho_{\uparrow\uparrow}(\vec{r})-\rho_{\downarrow\downarrow}(\vec{r})}. \tag{4}$$

These new degrees of freedom complicate the mean-field equations and lead to an exchange-correlation potential $\hat{V}^{\mathrm{xc}}$ in the form of a complex matrix in spin space

$$\hat{V}^{\mathrm{xc}}=\frac{1}{2}(V_{\uparrow}^{\mathrm{xc}}+V_{\downarrow}^{\mathrm{xc}})\hat{1}+\frac{1}{2}(V_{\uparrow}^{\mathrm{xc}}-V_{\downarrow}^{\mathrm{xc}})\hat{\vec{\sigma}}\cdot\vec{d}, \tag{5}$$

where $\vec{d}$ is a position-dependent unit vector along the direction of the vector $[\mathrm{Re}\,\rho_{\uparrow\downarrow}(\vec{r}),\mathrm{Im}\,\rho_{\uparrow\downarrow}(\vec{r}),\rho_{\uparrow\uparrow}(\vec{r})-\rho_{\downarrow\downarrow}(\vec{r})]$. The presence of the second term in the exchange-correlation potential allows a general coupling of the up and down components of the spinor wave functions. To interpret the magnetic properties, we compute the vector magnetization density $\vec{m}(\vec{r})$ by expressing the spin-density matrix in the form

$$\hat{\rho}(\vec{r})=0.5[n(\vec{r})\hat{1}+\vec{m}(\vec{r})\cdot\hat{\vec{\sigma}}]. \tag{6}$$

We associate magnetic moments with individual atoms by integrating each component of $\vec{m}(\vec{r})$ within a sphere centered on the ions, giving us the local magnetic moment vectors $\vec{\mu}_{\mathrm{at}}$. The integration radius is chosen to be one half of the smallest interatomic distance in each cluster to avoid overlap and the resulting spheres contain about 80–90 % of the magnetization density. Taking a larger radius for more distant atoms has a negligible effect on the orientation of their magnetic moment, although its magnitude becomes somewhat bigger. Due to the varying integration radius, however, magnitudes of local magnetic moments from different clusters cannot be compared easily.

As usual, we only treat the valence electrons explicitly, taking care of the ionic core with a pseudopotential approximation. We use the relativistic pseudopotential from Goedecker and co-workers,[28] which contains a local part plus a sum of separable Gaussians, optimized to represent a transferable nonlocal pseudopotential on a coordinate mesh. The multiplication of the wave functions with the nonlocal part can be limited to a small region around the ions as the radial projectors fall off rather quickly. However, 20 integrations within the covalent radius of each atom need to be performed to correctly account for nonlocal effects in chromium. The energetics at small ionic separations inside the clusters further requires us to include the $3s$ and $3p$ semicore electrons into the variational space. Our pseudopotential also includes spin-orbit terms that fix the orientation of the total magnetization M to the ionic structure, thus giving rise to magnetic anisotropy. The implementation of the $\vec{L}\cdot\vec{S}$ operator is not too costly because we have to deal with a complex spinor structure anyway. Spin-orbit effects enable us to test the validity of the usually applied atomic-sphere approximation by studying the intra-atomic dispersion.[29]

We have carried out an unconstrained structural search by fully optimizing electronic and ionic degrees of freedom. To find the ground state and stable isomers, the ionic positions were computed via Monte Carlo sampling applying the technique of simulated annealing. After some Metropolis steps, the electronic wave functions are updated with Kohn-Sham iterations. The optimization of the ionic geometry involves a minimization of the one-ion energies and is explained in detail in Ref. 30. The static Kohn-Sham equations are solved in a combined coordinate and momentum space representation by using an efficient damped gradient iteration.[31] Local operators are applied on coordinate space wave functions while the kinetic energy and the action of the spin-orbit operator are computed in momentum space applying fast Fourier techniques. The Poisson equation is solved via the FALR (Fourier analysis under special consideration of long range terms) method.[31] As it is more convenient for most physical observables, electronic wave functions and densities are stored on a three-dimensional coordinate space mesh. We perform our calculations in a cubic box with a mesh spacing of 0.32 a.u. and up to 64 grid points in each direction. We checked that the mesh size was big enough to avoid artifacts from the boundaries. A detailed description of our numerics can be found in Ref. 32.

III. RESULTS AND DISCUSSION

Before discussing our results, we mention some of the various tests we performed in order to increase our confidence in the Hamiltonian and its numerical implementation. The dimer plays a key role in the description of small chromium clusters. It is known that its subtle electronic properties demand a high accuracy of the Cr-Cr interactions and the numerical representation.[21] By applying the pseudopoten-

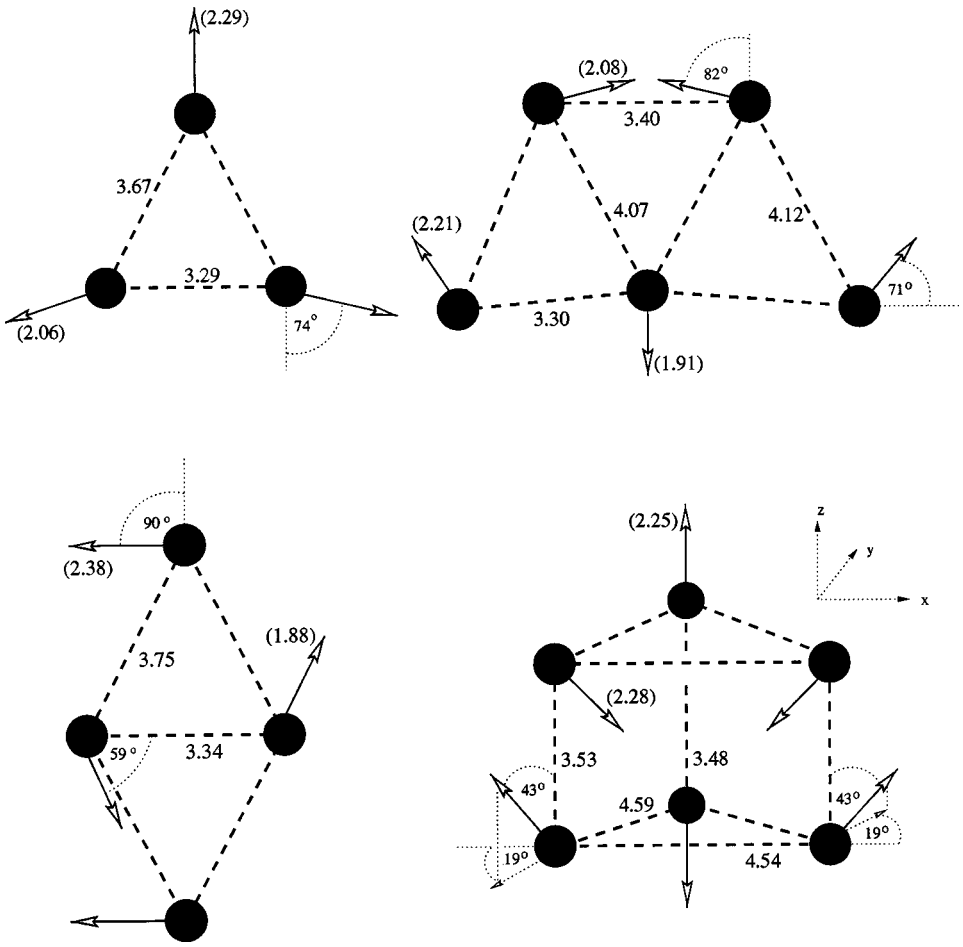

FIG. 1. Geometric and magnetic structures for the energetically lowest noncollinear configurations of Cr_N, $3 \leqslant N \leqslant 6$. The local magnetic moments, including their angles with respect to the x and z axes, are indicated by arrows. The interatomic distances are shown in atomic units and the magnitudes of the local magnetic moments $|\vec{\mu}_{at}|$ (in units μ_B) are given in brackets.

tial in the semicore version, our binding energy (1.98 eV) and bonding length ($d_0 = 3.25$ a.u.) for the antiferromagnetic ground state were in good agreement with experimental results (1.56 eV $\pm$ 0.3 eV, $d_{exp} = 3.19$ a.u.) and previous all-electron or pseudopotential calculations.[21] The correct energetic order of the single-particle levels as a function of the intramolecular distance, the symmetry of the wave functions, and the properties of the ferromagnetic coupling ($d = 5.2$ a.u.) could be reproduced as well. The same holds for the bonding length of the CrO molecule that deviated from the experimental result by 1.3%. Additionally, we achieved degenerate d states up to a level of 1% and the correct energetic order of $3d$ and $4s$ levels in the chromium atom. The rotationally invariant spin-density theory was checked by letting the FE configuration of the dimer relax to the AF ground state. As in the collinear theory, all spins were initially restricted to point in the z direction. The wave functions and energies of the final result turned out to be identical with the ground state as computed in a separate collinear approach, although the quantization axis of both atoms had rotated by $\pm 90°$ during the iteration. This confirms the degeneracy of the electronic properties with respect to the orientation of their spin. Furthermore, we have been able to verify the result of Car and co-workers[13] concerning the noncollinear spin arrangement of Fe_3.

Our results for the energetically lowest noncollinear configurations of small chromium clusters Cr_N ($3 \leqslant N \leqslant 6$) are presented in Fig. 1. All structures except the one of Cr_4 represent ground states. The corresponding total magnetization is shown in Table I. Our geometric and magnetic structures are obtained by performing up to 50 full Monte Carlo

TABLE I. Total magnetization per atom M_{at} (in units μ_B) for the ground states of Cr_N and gain in binding energy ΔE_{nc} (in units eV/atom) with respect to their collinear counterparts. In case of a collinear ground state, the result for the energetically lowest noncollinear isomer is given in parentheses. The last column shows the corresponding magnetization from the collinear calculation of Cheng and Wang (Ref. 22).

N_{at}	Type	M_{at}	ΔE_{nc}	M_{at} (Ref. 22)
2	Collinear	0.0 (−)	0.0 (−)	0.0
3	Noncollinear	0.69	0.083	2.0
4	Collinear	0.0 (1.33)	0.0 (0.12)	0.0
5	Noncollinear	0.53	0.054	0.93
6	Noncollinear	0.0	0.022	0.33
7	Noncollinear	0.13	0.019	0.29
9	Noncollinear	0.09	0.015	0.22
12	Noncollinear	0.81	0.011	1.67
13	Noncollinear	0.60	0.008	1.06

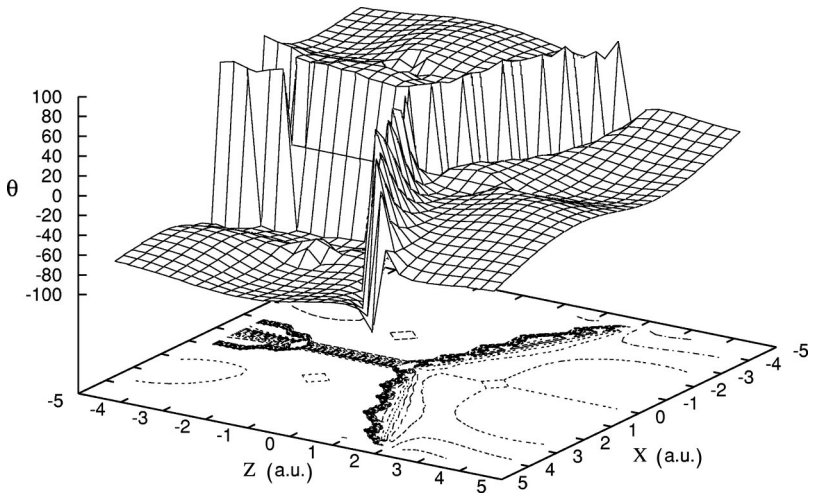

FIG. 2. Three-dimensional plot of the polar rotation angle θ (in degrees) from Eq. (4) within the plane defined by the ionic coordinates of Cr_3 (see Fig. 1). We also show the corresponding contour lines for θ with a step size of 10°. The ionic positions are at the center of the dashed squares.

runs per cluster starting from arbitrary ionic coordinates. A few thousand Kohn-Sham iterations are usually necessary to completely relax the electronic degrees of freedom. This is because the numerical convergence with respect to the direction of the local moments (governed by competing interatomic exchange interactions) is much slower than with respect to their magnitude, which is determined by stronger intra-atomic interactions.

The principle effect that leads to noncollinear arrangements in chromium clusters can best be demonstrated in Cr_3. Our calculation restricted to collinear spins gives a trimer that basically consists of a dimer plus a loosely attached third atom, very similar to the result of Cheng and Wang.[22] It is obviously impossible for the atoms to couple antiferromagnetically with all their neighbors at a time so that a FE interaction between two atoms becomes inevitable—a situation that we refer to in the following as frustration. The repulsive effect of the FE coupling at smaller distances pushes one atom away and results in a large interatomic distance of 4.97 a.u. If the noncollinear channel is accessible, however, the trimer is free to achieve the closest to AF-like coupling it can by rotating two local magnetic moments in the x-z plane (see Fig. 1). As the frustration is now reduced, the third atom comes much closer ($d=3.67$ a.u.) and enables a buildup of molecular orbits that enhances the total binding inside the trimer significantly. The associated reduction of $|\vec{\mu}_{\rm at}|$ to $2.29\mu_{\rm B}$ for the formerly isolated atom results in a decrease of $M_{\rm at}$ from $2\mu_{\rm B}$ to $0.69\mu_{\rm B}$. The energy difference with respect to the collinear ground state $\Delta E_{\rm nc}$ is 0.083 eV per atom (see Table I), which amounts to 7.8% of the binding energy of Cr_3. A look at the interatomic distances and the tilted local moments suggests that the dimer lost its dominant role. However, the fact that the ground state is not an equilateral triangle with angles of 120° between the local magnetic moments (this would equal the best possible AF-like coupling) indicates that some trace of the strong dimer binding from the collinear calculation still persists. Unlike the situation in Fe_3, the linear isomer of Cr_3 did not favor noncollinear spins.

The noncollinear spin structure of Cr_3 can be understood as a compromise between the energetically very favorable AF coupling and frustration. This can be seen easily with the very simple Hamiltonian $H=\beta\Sigma_{i<j}^{3}\vec{\sigma}_i\cdot\vec{\sigma}_j$ for three spins on an equilateral triangle. Here β is negative for AF coupling. In a collinear restriction, the lowest-energy state formed by a product wave function is $(\uparrow\uparrow\downarrow)$ with an energy expectation $\langle H\rangle=\beta$. Taking instead the state with 120° angles between the spin directions gives a lower energy of $\langle H\rangle=3/2\beta$. For higher atomic spins (as they occur in our numerical computations) the preference of the noncollinear configuration would, of course, become more pronounced due to the larger number of exchange interactions.

In Fig. 2 we show the rotation angle $\theta(\vec{r})$ in the x-z plane of the trimer, including its contour lines in steps of 10°. The azimuthal angle $\phi(\vec{r})$ is zero at any grid point due to the magnetic anisotropy energy although this quantity is rather small. But it seems that even a difference of a few meV per atom is enough to keep the magnetization inside the plane of the trimer, an observation that agrees with the findings of Ref. 11. The orientation of the magnetization density vector is remarkably uniform in the regions surrounding the ions: $\theta\simeq\pm 74°$ for the ions at $x=\pm 1.645$, $z=-1.64$, and $\theta=0°$ for the third ion at $x=0, z=1.64$. Besides a small oscillation of $\Delta\theta\simeq\pm 10°$ in these regions, θ varies significantly only right between them where the charge density is essentially zero. This is why a smaller integration radius only influences the magnitude of $\vec{\mu}_{\rm at}$ and not its orientation. The rapid change from $\theta=-90°$ to $\theta=90°$ (indicated by a very high density of the contour lines) is related to a spin flip in these interatomic regions. We find an intra-atomic spin dispersion of around 6° that partly comes from spin-orbit coupling. But the dispersion is also induced by the trend to an AF coupling with the neighbors. The same especially holds for the variation of the spin direction close to the domains of other atoms. The change of θ at the ionic positions (dashed squares) is an artifact of the pseudopotential approximation. A detailed analysis further shows that these features are common to all investigated chromium clusters.

The collinear ground state of Cr_4 was found to have a rectangular structure (not shown) with bonding lengths of

3.35 a.u. and 4.62 a.u. The double dimer structure of this geometry appears to be resistant to noncollinear effects as the distance of two atoms with parallel moments is very large (5.7 a.u.). But in the case of the lowest isomer, a rhombus, frustration becomes important again resulting in noncollinear spins (see Fig. 1). The argumentation follows the case of Cr_3, the triangles in Cr_4 are very similar and have only slightly larger bonding lengths. A higher total magnetization of $M_{at}=1.33\mu_B$ leads to an energy gain of 0.12 eV per atom with respect to the corresponding collinear state of the rhombus and halves the energy difference to the rectangular ground state. The isomer of Cr_4 is unique in that the energetically favored noncollinear configuration has a bigger total magnetization than its collinear counterpart. The magnitudes of $\vec{\mu}_{at}$, however, were similar in both cases. It is also noteworthy that the rhombus structure provides angles between the local moments of almost exactly 120°, although the bondings are not equivalent. This seems to be related with the larger moments of the furthermost atoms ($\Delta|\vec{\mu}_{at}|=0.5\mu_B$).

The properties of the noncollinear ground state of Cr_5 can be understood if one considers the pentamer as consisting of three triangles. Although the bonding lengths are bigger, each of these triangles exhibits the same basic features as Cr_3 and the local moments are again arranged in such a way that the best possible AF-like coupling is achieved. We observe that the magnitude of $\vec{\mu}_{at}$ decreases with increasing coordination number, as can be seen from the center atom with $|\vec{\mu}_{at}|=1.91\mu_B$. Note that the reflection symmetry of the geometry is the same as the symmetry of the magnetization. The gain in binding energy with respect to the best collinear state is 0.054 eV per atom (=3.7% of the binding energy), which is less than for the trimer. But the total magnetization is again clearly reduced from 1.03 to $0.53\mu_B$ per atom. The lowest isomer is a bipyramid with a noncollinear spin structure as well and $M_{at}=0.79\mu_B$. Its energy difference of 0.6 eV to the ground state is 0.25 eV higher than in the collinear case. Cr_5 is the only cluster we found where the noncollinear and collinear geometries differ by more than just a variation of the bonding lengths. Our lowest collinear state looks similar to the geometry of Cheng and Wang and has a $2v$ symmetry. However, its total magnetization of $1.05\mu_B$ is somewhat higher than their result of $0.93\mu_B$.

The shape of Cr_6, on the other hand, resembles the collinear one very closely. Cr_6 is the smallest cluster that displays a fully three-dimensional geometric and magnetic structure in the ground state (Fig. 1). It consists of three dimers distributed over two triangles in which frustration sets in. Each of the $\vec{\mu}_{at}$ is exactly antiparallel to the moment of its partner atom in the dimer. The azimuthal angles are $\phi=\pm 19°$ for the atoms in the foreground and $\phi=0°$ for the ones in the background that are slightly closer. The bonding lengths in the triangles are about 6% shorter than in the collinear case and the dimer distances are somewhat bigger. It is important to note that in spite of a vanishing total magnetization and although the dimer seems to recover a certain influence, tilted spins are still energetically favored. However, the gain of $\Delta E_{nc}=0.022$ eV per atom only accounts for 1.4% of the binding energy of Cr_6. This indicates that the impact of noncollinear effects on the energetics becomes

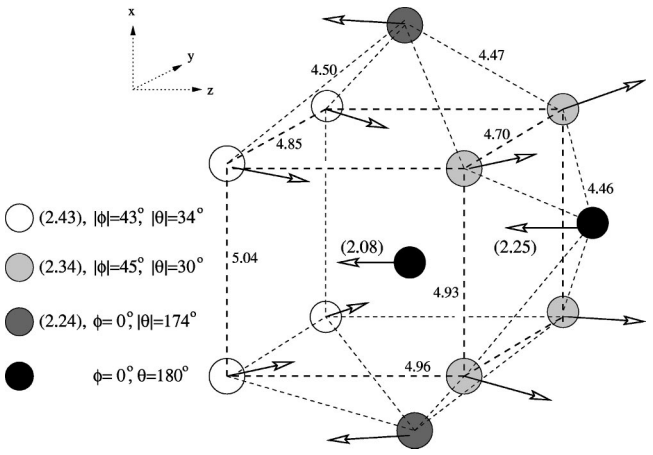

FIG. 3. Geometric and magnetic structure of the noncollinear ground state of Cr_{12}. The notation follows the one from Fig. 1. The magnetic moments of the lighter-colored atoms show a dispersion in the positive z direction, whereas the darker atoms almost exactly point in the negative z direction. We also display the absolute values of the azimuthal and polar angles as well as the magnitudes of $\vec{\mu}_{at}$ for all four groups of atoms.

gradually smaller with rising cluster size. Further calculations for Cr_7 and Cr_9 confirm this trend and predict that the noncollinear geometries essentially equal the collinear ones for $N_{at}\geqslant 6$. On the other hand, our results so far show that noncollinear spin configurations considerably reduce the total magnetization of the ground states although it might not be reflected too much in the binding energy. This can be understood in terms of the competing interatomic exchange interactions that involve only small energy changes during the rotation of local moments (see above).

We shall finally discuss how noncollinear effects might provide a way to ameliorate the disagreement between the measured total magnetic moments of Cr_N ($N\geqslant 9$) by Bloomfield and co-workers[23] and previous theoretical results.[22,24] The Stern-Gerlach experiment extracted an upper bound for M_{at}, $M_{at}<0.77\mu_B$, assuming a superparamagnetic behavior of the chromium clusters. Earlier calculations, however, report values for the magnetization of some clusters that are much higher.[24] The values from Cheng and Wang for Cr_{12} ($M_{at}=1.67\mu_B$) and Cr_{13} ($M_{at}=1.06\mu_B$) also exceed the experimental limit. The trend from smaller clusters gives one the hope that noncollinear effects might reduce the difference. However, an unconstrained simultaneous optimization of electronic and ionic degrees of freedom surpasses our computational resources for clusters as large as Cr_{12}. Instead, we start the optimization procedure from the geometries of Cheng and Wang. This is a reasonable approach in the light of the very good agreement with our collinear structures and the small changes in geometry that are induced by noncollinear spins. Our final magnetic and geometric configuration of Cr_{12} is shown in Fig. 3. The free relaxation leads to a shortening of the bonding lengths between the corner atoms of about 5% and slightly bigger distances of the capping atoms but the bulklike bcc structure of the collinear geometry clearly persists. The z components of the local magnetic moments vary on alternating x-y planes, but only the moments of the corner atoms have significant x and y components. All the spins of the lightest-colored corner at-

oms point inside the cube towards the central atom, whereas the spins of the slightly darker corner atoms point outside and away from the next atom. This dispersion is related to some frustration of the corner atoms in connection with the preferred AF coupling to the moments of their nearest neighbors (darker atoms). A magnetic arrangement like that can be seen as a precursor to the bulk behavior in form of a spin-density wave that is achieved by an almost antiparallel order between neighboring layers. It should be noted that more compact and thus more frustrated structures different from the bcc-like geometry might result in a very different magnetic behavior. This question is presently being investigated.

The tilted spins of the corner atoms ($\phi=\pm 43°$, $\theta=\pm 34°$ and $\phi=\pm 45°$, $\theta=\pm 30°$) have pairwise opposite x and y components so that the sum of their net moments in positive z direction is reduced. The moments of the darker atoms, however, show almost no dispersion in negative z direction. All this results in a much smaller total magnetization of $M_{\mathrm{at}}=0.81\mu_{\mathrm{B}}$, which is now very close to the experimental limit (although the geometry is almost identical to the collinear case). The remarkable reduction of $\Delta M_{\mathrm{at}}=-0.86\mu_{\mathrm{B}}$ is associated with $\Delta E_{\mathrm{nc}}=0.011$ eV per atom, which equals only 0.5% of the binding energy of Cr_{12}. A very similar situation leads to $M_{\mathrm{at}}=0.60\mu_{\mathrm{B}}$ in the case of Cr_{13}, a value that is even below the experimental limit. The noncollinear gain amounts to $\Delta E_{\mathrm{nc}}=0.008$ eV per atom underlining the trend to a gradually decreasing influence of noncollinear effects on the binding energy. We can conclude from our analysis that the total magnetization of Cr_{12} and Cr_{13} as obtained with the general LSDA represents a considerable improvement with respect to the experiment.

IV. CONCLUSIONS

We present a study of noncollinear effects in antiferromagnetically coupled clusters by applying the general, rotationally invariant LSDA for the electronic degrees of freedom. Their interaction with the ions is described in terms of a relativistic, nonlocal pseudopotential that has been thoroughly tested. The magnetic and geometric structures are obtained by employing a simulated annealing technique for the ionic optimization together with interlaced Kohn-Sham iterations that update the wave functions simultaneously.

Our collinear configurations, which we use in order to extract the effect of noncollinear spins, agree very well with the results of Cheng and Wang.[22] We find that all investigated chromium clusters show a pronounced trend to noncollinear spin configurations. This is caused by a subtle interplay between the preferred magnetic order and frustration, a situation that can in principle occur in all clusters of elements that favor antiferromagnetic spins. Therefore our considerations appear to be of a more general nature although the special properties of chromium indicate that noncollinear effects could be less dramatic in other transition metals. The results for $N_{\mathrm{at}}\leqslant 13$ show that the influence of noncollinearity on various observables becomes gradually smaller with rising cluster size. Induced changes of the cluster geometry are generally restricted to an alteration of the bonding lengths, with the exception of Cr_5. However, we observe a universal reduction of the total magnetization that is significant even in those clusters for which a variation of the magnetic distribution is not clearly reflected in the binding energy any more (Cr_{12} and Cr_{13}). This effect is related to the small energetic changes that occur during the rotation of local moments, an aspect that makes a proper convergence of the Kohn-Sham iteration very time consuming. Furthermore, our findings show that tilted spins due to frustration can even be favored when the total magnetization vanishes (Cr_6) or the corresponding ground state is collinear like in Cr_4. The free variation of the spin quantization axis finally leads to a better agreement with the experiment concerning the total magnetization of Cr_{12} and Cr_{13}. It can be concluded that noncollinear effects appear to be an important ingredient for a deeper understanding of the subtle magnetic properties in transition-metal clusters.

ACKNOWLEDGMENTS

One of the authors (C.K.) has been supported by the DAAD (German Academic Exchange Service), Grant No. D/98/14581. We also thank Ana Proykova, Sanjay Reddy, Paul-Gerhard Reinhard, Louis Bloomfield, and Lai-Sheng Wang for many useful and encouraging discussions.

[1] D. C. Douglass, A. J. Cox, J. P. Bucher, and L. A. Bloomfield, Phys. Rev. B **47**, 12 874 (1993); S. E. Apsel, J. W. Emmert, and L. A. Bloomfield, Phys. Rev. Lett. **76**, 1441 (1996).

[2] I. M. L. Billas, J. A. Becker, and W. A. de Heer, Z. Phys. D **24**, 325 (1993); I. M. L. Billas, A. Châtelain, and W. A. de Heer, Science **265**, 1682 (1994).

[3] G. Ganteför and W. Eberhardt, Phys. Rev. Lett. **76**, 4975 (1996).

[4] H. Wu, S. R. Desai, and L. Wang, Phys. Rev. Lett. **77**, 2436 (1996).

[5] B. V. Reddy, S. N. Khanna, and B. I. Dunlap, Phys. Rev. Lett. **70**, 3323 (1993); M. Menon, J. Connolly, N. N. Lathiotakis, and A. N. Andriotis, Phys. Rev. B **50**, 8903 (1994).

[6] G. F. Bertsch, N. Onishi, and K. Yabana, Z. Phys. D **34**, 213 (1995); V. Visuthikraisee and G. F. Bertsch, Phys. Rev. A **54**, 5104 (1996).

[7] J. Guevera, F. Parisi, A. M. Llois, and M. Weissmann, Phys. Rev. B **55**, 13 283 (1997); Q. Sun, G. Wang, J. Z. Yu, Z. Q. Li, and J. T. Weng, J. Phys. I **7**, 1233 (1997).

[8] A. N. Andriotis, N. N. Lathiotakis, and M. Menon, Europhys. Lett. **36**, 37 (1996).

[9] A. J. Cox, J. G. Louderback, S. E. Apsel, and L. A. Bloomfield, Phys. Rev. B **49**, 12 295 (1994); P. Villaseñor-González, J. Dorantes-Dávila, H. Dreyssé, and G. M. Pastor, *ibid.* **55**, 15 084 (1997).

[10] S. E. Apsel, J. W. Emmert, J. Deng, and L. A. Bloomfield, Phys. Rev. Lett. **76**, 1441 (1996); I. M. L. Billas, A. Châtelain, and W. A. de Heer, J. Magn. Magn. Mater. **168**, 64 (1997); F. Aguilera-Granja, S. Bouarab, M. J. López, A. Vega, J. M. Montejano-Carrizales, M. P. Iñiguez, and J. A. Alonso, Phys. Rev. B **57**, 12 469 (1998).

[11] G. M. Pastor, J. Dorantes-Dávila, S. Pick, and H. Dreyssé, Phys. Rev. Lett. **75**, 326 (1995); J. Dorantes-Dávila, and G. M. Pastor, *ibid.* **81**, 208 (1998).
[12] P. J. Jensen and K. H. Bennemann, Z. Phys. D **35**, 273 (1995); J. Zhao, X. Chen, Q. Sun, F. Liu, and G. Wang, Europhys. Lett. **32**, 113 (1995); P. Borrmann, B. Diekmann, E. R. Hilf, and D. Tománek, Surf. Rev. Lett. **3**, 463 (1996); M. Respaud, J. M. Broto, H. Rakoto, A. R. Fert, L. Thomas, B. Barbara, M. Verelst, E. Snoeck, P. Lecante, A. Mosset, J. Osuna, T. Ould Ely, C. Amiens, and B. Chaudret, Phys. Rev. B **57**, 2925 (1998).
[13] T. Oda, A. Pasquarello, and R. Car, Phys. Rev. Lett. **80**, 3622 (1998).
[14] M. Uhl, L. M. Sandratskii, and J. Kübler, Phys. Rev. B **50**, 291 (1994).
[15] M Liebs;, K. Hummler, and M. Fähnle, Phys. Rev. B **51**, 8664 (1995); R. Lorenz, J. Hafner, S. S. Jaswal, and D. J. Sellmyer, Phys. Rev. Lett. **74**, 3688 (1995).
[16] R. Lorenz and J. Hafner, Phys. Rev. B **58**, 5197 (1998).
[17] A. Schreyer, C. F. Majkrzak, T. Zeidler, T. Schmitte, P. Bödeker, K. Theis-Bröhl, A. Abromeit, J. A. Dura, and T. Watanabe, Phys. Rev. Lett. **79**, 4914 (1997); R. S. Fishman, *ibid.* **81**, 4979 (1998).
[18] S. Demuynck, J. Meerschaut, J. Dekoster, B. Swinnen, R. Moons, A. Vantomme, S. Cottenier, and M. Rots, Phys. Rev. Lett. **81**, 2562 (1998).
[19] P. Alvarado, J. Dorantes-Dávila, and G. M. Pastor, Phys. Rev. B **58**, 12 216 (1998).
[20] E. Viitala, J. Merikovski, M. Manninen, and J. Timonen, Phys. Rev. B **55**, 11 541 (1997).
[21] B. Delley, A. J. Freeman, and D. E. Ellis, Phys. Rev. Lett. **50**, 488 (1983); J. Bernholc and N. A. W. Holzwarth, *ibid.* **50**, 1451 (1983); L. Andersson, Chem. Phys. Lett. **237**, 212 (1995).
[22] H. Cheng and L. Wang, Phys. Rev. Lett. **77**, 51 (1996).
[23] D. C. Douglass, J. P. Bucher, and L. A. Bloomfield, Phys. Rev. B **45**, 6341 (1992).
[24] G. M. Pastor, J. Dorantes-Dávila, and K. H. Bennemann, Phys. Rev. B **40**, 7642 (1989); K. Lee and J. Callaway, *ibid.* **49**, 13 906 (1994).
[25] U. Barth and L. Hedin, J. Phys. C **5**, 1629 (1972).
[26] J. P. Perdew and Y. Wang, Phys. Rev. B **45**, 13 244 (1992).
[27] J. Kübler, K.-H. Höck, J. Sticht, and A. R. Williams, J. Phys. F **18**, 469 (1988).
[28] C. Hartwigsen, S. Goedecker, and J. Hutter, Phys. Rev. B **58**, 3641 (1998).
[29] L. Nordström and D. J. Singh, Phys. Rev. Lett. **76**, 4420 (1996).
[30] C. Kohl, Ph.D. thesis, Erlangen-Germany, 1997.
[31] G. Lauritsch and P.-G. Reinhard, Int. J. Mod. Phys. C **5**, 65 (1994).
[32] C. Kohl, B. Fischer, and P.-G. Reinhard, Phys. Rev. B **56**, 11 149 (1997); C. Kohl, F. Calvayrac, P.-G. Reinhard, and E. Suraudi, Surf. Sci. **405**, 74 (1998).